Performance of Superconducting Quantum Computing Chips under Different Architecture Designs

Wei Hu* · **Yang Yang*** · **Weiye Xia** ·
Jiawei Pi · **Enyi Huang** · **Xin-Ding**
Zhang · **Hua Xu**

Abstract Existing and near-term quantum computers can only perform two-qubit gates between physically connected qubits. Research has been done on compilers to rewrite quantum programs to match hardware constraints. However, the quantum processor architecture, in particular the qubit connectivity and topology, still lacks enough discussion, while it potentially has a huge impact on the performance of the quantum algorithms. We perform a quantitative and comprehensive study on the quantum processor performance under different qubit connectivity and topology. We select ten representative design models with different connectivities and topologies from quantum architecture design space and benchmark their performance by running a set of standard quantum algorithms. It is shown that a high-performance architecture almost always comes with a design with a large connectivity, while the topology shows a weak influence on the performance in our experiment. Different quantum algorithms show different dependence on quantum chip connectivity and topologies. This work provides quantum computing researchers with a systematic approach to evaluating their processor design.

* Wei Hu and Yang Yang contributed equally to the work.
Corresponding author: Hua Xu hua.xu@kfquantum.com · Xin-Ding Zhang

Wei Hu · Yang Yang · Weiye Xia · Hua Xu
Kunfeng Quantum Technology Co., Ltd, Shanghai, China.
E-mail: wei.hu@kfquantum.com
E-mail: yang.yang@kfquantum.com
E-mail: hua.xu@kfquantum.com

Jiawei Pi · Enyi Huang · Xin-Ding Zhang
Guangdong Provincial Key Laboratory of Quantum Engineering and Quantum Materials,
School of Physics and Telecommunication Engineering, South China Normal University,
Guangzhou 510006, China
E-mail: xdzhang2000@gmail.com

1 Introduction

Inspired by the vast potential applications and superb computing power, quantum computing (QC) has attracted rapidly growing interest of researchers in the past decades. There are multiple potential quantum computing hardware systems under study. Among those systems, superconducting qubits [1–5], and trapped ions [6, 7] have been leading the technology advancement of the QC on the functionality and technology maturity. Both systems have been able to integrate qubits on the order of tens of qubits to nearly one hundred [8–11], and fully programmable multi-qubit machines have been built based on these systems. Such machines provide users with a high-level interface that enables them to implement arbitrary quantum circuits. This makes it possible for the first time to test quantum computers irrespective of their particular physical implementation.

Since there are multiple physical realizations of QC and different implementation methods of physical systems, quantum computers not only have different number of qubits, but also different connectivity and different gating operation between qubits. How to accurately compare and evaluate the performance of quantum chips is then a challenge, as well as a core question. To tackle this question, IBM proposed the concept of Quantum Volume [12], and other research groups have also come up with methodologies to evaluate and benchmark quantum chips [12, 13].

It has been widely agreed that the capacity of a quantum computer is not just determined by the number of qubits [14]. There are many other factors, such as qubit quality including single-qubit coherent time, single-qubit gating fidelity and two-qubit gating operation fidelity, etc, and chip architecture including qubit-qubit connectivity, and qubit-qubit topology layout. In addition to the number of qubits, the researchers have been mostly focused on the quality of those qubits when discussing the performance of quantum computers.

Recently, there are only few studies on the quantum chip architecture, especially *connectivity* and *topology*. The quantified definition of connectivity will be given in Sec. 2.2 while the word topology here refers to the topological property of qubits network and has nothing to do with topological quantum computing. Norbert M. Linke et al. have compared two quantum computing architectures, superconducting transmon system and ion trap system. In their research, they pioneered the impact of connectivity on the quantum processor performance, and claimed achieving high connectivity for a large-scale superconducting processor is an important, but still open question [15]. On a partially connected architecture, the compiler must dynamically map logical qubits in an arbitrary quantum circuit to physical qubits on the quantum chip. This problem is known as qubit allocation or qubit mapping, which multiple methods have been developed by researchers [16–18].

Till now, there still lacks systematic and comprehensive study on the architecture of the quantum processor and its related connectivity and topology to answer the following questions: how connectivity strength and position, as well as the topology will impact the performance of a quantum processor? What will the overhead of a certain connectivity quantum processor be?

In this paper, we have done a quantitative and comprehensive study on these questions. We studied the design of quantum chip architecture, including qubit-qubit connectivity and qubit topology layout, and analyzed the performance of different architecture designs both qualitatively and quantitatively. Our study will be helpful to give quantitative analysis and comparison of different QC systems. Besides, this study will dramatically help the QC researchers to design their chips. With a systematic method to evaluate the chip performance, the QC researchers can balance the connectivity requirement and other restrictions when designing the QC chips, to achieve the best performance in their design space.
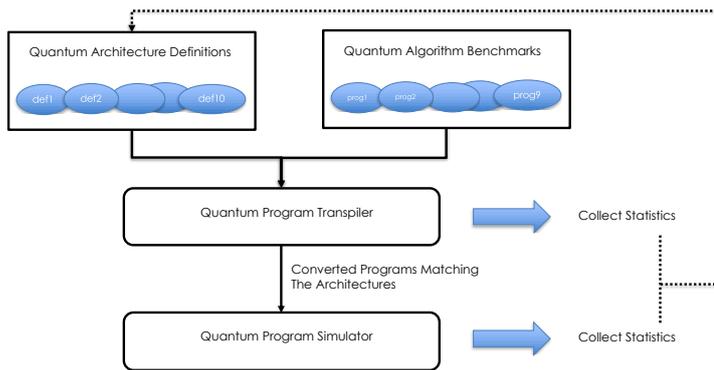
Whereas the quantum computers considered here are still small scale and their capabilities do not currently reach beyond demonstrative algorithms, this line of inquiry can still provide useful insights into the performance of existing systems and the role of architecture in quantum computer design. These findings will be crucial for the realization of more advanced future incarnations of the present technologies.

The organization of the paper is as follows:

1. Describe the overall experimental setup. It includes the workflow of the experiment, and how we design the quantum algorithm benchmark suite for the evaluation.

2. Based on the results of different chip architectures, we perform the analysis and evaluate the impact of qubit connectivity on the performance of the benchmarks.

3. Finally, based on the analysis, we propose some guidelines on the quantum processor design. Moreover, some possible future topics have also been proposed. The method developed in the paper will be a great contribution for QC designers.

2 Experiment

The workflow of our experiment is depicted in Fig. 1. To study the performance of different quantum architectures, we evaluate 10 representative architectures based on existing designs, by running 9 well-known quantum algorithm implementations as benchmarks. We make use of IBM Qiskit to transpile and simulate the benchmarks on every architecture. The quantitative analysis of the performance metrics collected offers valuable guidance to quantum chip designers.

Fig. 1 Experiment setup and overall workflow.

2.1 Selection of Algorithms

Inspired by a previous work [18], we select 5 representative quantum algorithms for testing, shown in Table. 1. Most of these algorithms are commonly viewed as classical quantum algorithms, including Quantum Fourier Transfrom (QFT), Quantum Phase Estimation (QPE), Surface Code Error Correction (SCE). Additionally, the problem of one dimensional Ising model with six qubits is chosen as another test algorithm.

The QFT and QPE are the cornerstones of many other algorithms, such as Shor's algorithm, Quantum Machine Learning algorithms and Quantum option pricing algorithms [19–22]. Quantum error correction (QEC) is a central topic in quantum information theory so we choose two test algorithms, namely QEC with Steane-enlargement and the surface code [23,24]. The surface code is used for fault-tolerant quantum computation. The code requires a 2D square-lattice of qubits with only the nearest neighbor interactions. The Ising model is one of the most studied models in statistical physics, like the hydrogen atom model in quantum mechanics [25].

For the algorithms we have selected, we create their implementations including qft_{12}, qft_{16}, qft_{30}, qft_{32}, qpe_{15}, $steane_{25}$, $surface_{15}$, $surface_{25}$, $ising_6$, where the subscript indicates the number of qubits used and the meaning of abbreviations is summarized in Table. 1.

abbreviations	algorithms
qft	quantum fourier transform
qpe	quantum phase estimation
$steane$	quantum error-correcting codes obtained by using Steane-enlargement
$surface$	quantum error correction with the surface code
$ising$	one dimensional Ising model

Table 1 Abbreviations.

2.2 Selection of Architectures

There are several candidate technologies to implement QC physically, including superconducting quantum circuit [26], ion trap [27,28], quantum dot [29], neutral atom [30,31], etc. Among them, the superconducting quantum circuit is the most promising one with IBM and Google as two leading players in this field. IBM has built the first commercialized quantum computing platform since 2015. Google announced a 72-qubit chip in 2018 and claimed quantum supremacy on a 53-qubit quantum processor in 2019 [32]. There are two well-known types of connectivity in quantum chip design, Low Connectivity (LC) and Linear Nearest Neighbor (LNN). The former is adopted by IBM's Almaden, Boeblinden, Singapore, Johannesburg, Poughkeepsie and Tokyo architectures, while the latter, another popular design, is used by Google in their 53- and 72-qubit systems [32]. Google Sycamore chooses a square-like structure and Google Bristlecone is a rectangle-like 6×12 lattice structure.

Inspired by these pioneer designs, we propose two types of architecture models of 32 qubits that meet physics constraints, shown in Fig. 2. They demonstrate the differences in topology and connectivity. The first five chips labeled r_1 through r_5 have a rectangle-like topology, whereas the other five labeled s_1 through s_5 have a square-like topology. r_1 is a fully connected variant based on LNN. r_2 is the IBM Q 20 Tokyo architecture. r_3 is the commonly used LNN, adopted by Google Sycamore and Bristlecone. r_4 and r_5 are similar to the architecture of IBM Almaden, Boeblinden, Singapore, Johannesburg and Poughkeepsie. The connectivity of r_4 and r_5 are the same but the positions of connections are slightly different. These five architectures give four different connectivities. s_1 through s_5 are the square-like counterparts of r_1 through r_5. The square topology is a more symmetrical layout with a length/width aspect ratio close to 1. Compared with the square-like topology, the rectangular-like topology is a more asymmetrical layout with different aspect ratios. For instance, the aspect ratio is 32 for 32×1 lattice topology (single-chain topology), and the aspect ratio is 8 for 16×2 lattice topology. In this article, the rectangular-like topology we discussed has aspect ratio of 2 with 8×4 lattice topology.

Since there are the same numbers of qubits (vertices) in the rectangle- and square-like circuit, connectivity c can be quantified as follows,

$$c = \frac{n_{con}}{n_{full}}, \tag{1}$$

where n_{con} and n_{full} indicate the number of connected edges and the number of edges in the fully connected architecture, respectively, in these two corresponding configurations. The values of connectivity can be found in Table 2. It is noticeable that $c_{r_1} > c_{r_2} > c_{r_3} > c_{r_4} = c_{r_5}$, and $c_{s_1} > c_{s_2} > c_{s_3} > c_{s_4} = c_{s_5}$, and it is possible that the corresponding performance would follow a similar relation. Our experiment will be able to validate this intuition. We will also try to answer other non-intuitive questions, such as how the rectangle-like topol-

ogy compares to the square-like topology, which of r_4 or r_5 is better, which of s_4 or s_5 is better, etc.

	r_1	r_2	r_3	r_4	r_5	s_1	s_2	s_3	s_4	s_5
n_{con}	188	148	104	80	80	188	152	104	78	78
c	1.0	0.79	0.55	0.43	0.43	1.0	0.81	0.55	0.41	0.41

Table 2 The connectivity in the rectangle-like and square-like architectures. n_{con} indicates No. of connected edges and c represents the connectivity.

In summary, we have two types of architecture topologies and for each topology, there are five levels of connectivities. These settings are essential to reveal how topology and connectivity impact the performance of QC processors.
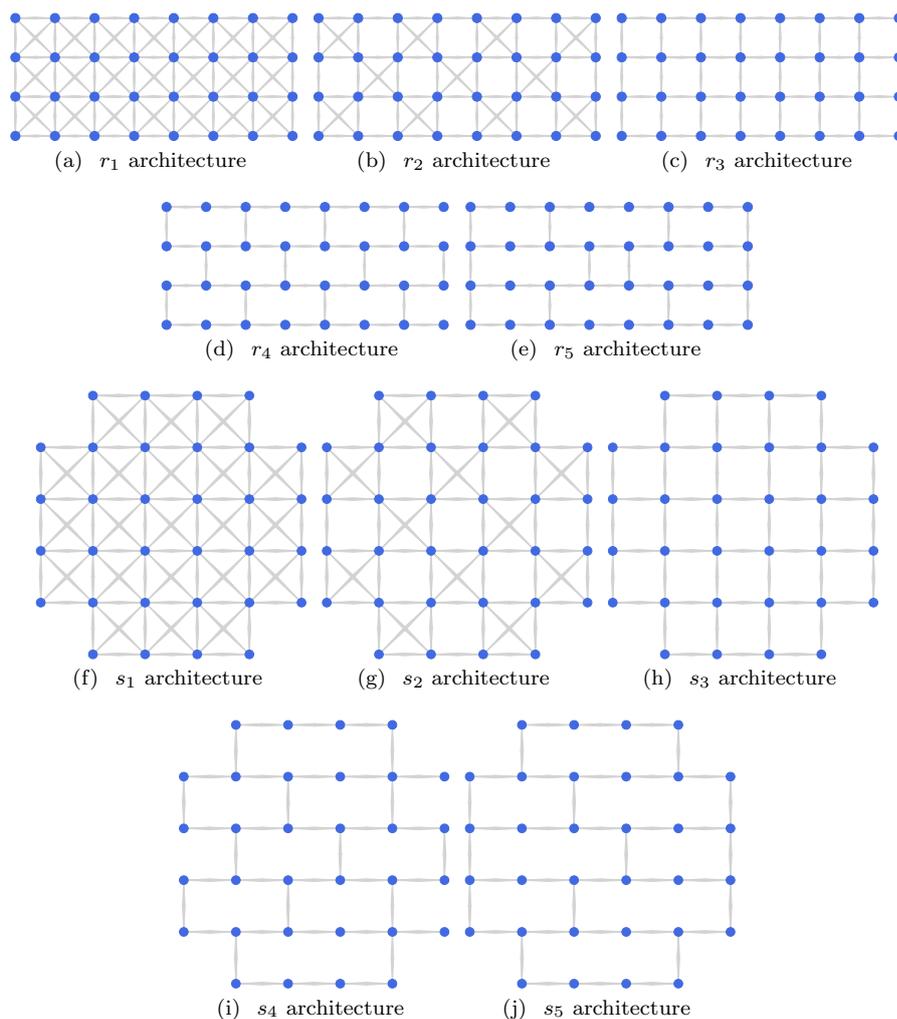
2.3 Running the Experiment

To evaluate the performance of each architecture, we make use of the IBM Qiskit transpiler [33] that rewrites quantum programs to match the architecture's qubit connectivity and its native quantum gates. We then run the IBM Qiskit simulator on the original benchmark programs as well as the output programs. We collect data as performance metrics, which will be discussed in Sec. 3.

To draw a fair comparison between architectures, ideally the transpiler should find the optimal program equivalent to the input. However, since this problem is NP-complete [16], finding the optimal result is not always feasible. Here we first summarize the transpilation process, and then explain our criteria of selecting the output program that best represents the performance of a benchmark on an architecture.

A quantum program usually assumes all-to-all qubit connectivity, and freely uses any quantum gates allowed by the programming language. In reality, a target quantum chip only supports a handful of quantum gates, and can only perform two-qubit gates between physically connected qubits. Barenco et al. proved that an arbitrary quantum gate can be decomposed into single-qubit gates and two-qubit CNOT gates, or any set of so-called universal quantum gates [34]. To work around qubit connectivity limitations, the transpiler searches for and inserts SWAP operations when necessary till an efficient mapping from logical qubits to physical qubits on the quantum chip are achieved.

Qiskit ships two qubit mapping algorithms, the original, default one, and a newer one called SABRE, proposed by Li et al [18]. In addition to transformations for the target architecture, Qiskit also has transformations aimed at optimizing the performance. Similar to classical compilers, Qiskit comes with four optimization levels from 0 to 3, although more optimizations do not always give better performance.

(a) r_1 architecture   (b) r_2 architecture   (c) r_3 architecture

(d) r_4 architecture   (e) r_5 architecture

(f) s_1 architecture   (g) s_2 architecture   (h) s_3 architecture

(i) s_4 architecture   (j) s_5 architecture

Fig. 2 The schematics of five rectangle-like and five square-like architectures.

With 2 choices of qubit mapping algorithm and 4 levels of optimization, Qiskit provides 8 combinations. For every pair of benchmark program and target architecture, we run each of the 8 mapping/optimization combinations 10 times to produce 80 output programs in total, and then select the best output according to the scoring function below. The reason we run each combination multiple times is that the output can differ over repeated runs, caused by randomization introduced to find approximate solutions to the NP-complete qubit mapping problem.

As the target architecture is only hypothetical with no real hardware, we propose a scoring function that estimates the error rate of a program. Because

noisy quantum gates introduce errors, it is important to minimize the number of gates to reduce the accumulated errors. It is also important to minimize the circuit depth so that all the computation can be accomplished before the qubits lose their quantum states. This reasoning leads to the following scoring function s that estimates the overall error rate of a quantum circuit,

$$s = \beta \cdot \left[1 - (1 - \frac{\sum E_{r_i} N_i}{\sum N_i})^{depth}\right], \tag{2}$$

in which the term on the right-hand side corresponds to error rates contributed by circuit depth. N_i is the number of a certain gate, and E_{r_i} is the corresponding error rate of this gate. β is a coefficient determined by data from real chips. $\frac{\sum E_{r_i} \cdot N_i}{\sum N_i}$ is the average error rates, replacing the error rate of each individual layer for simplicity. In this paper, given that $\frac{\sum E_{r_i} \cdot N_i}{\sum N_i} \ll 1$ and drop the constant β, a simplified formula of Eq. 2 is used to estimate the overall error rates of a quantum circuit, which is written as the multiplication of circuit depth and average error rate of each circuit layer,

$$s = depth \cdot \frac{\sum E_{r_i} \cdot N_i}{\sum N_i}. \tag{3}$$

The Eq. 3 above has been adopted in our study with IBM's error rate data, namely the single-qubit gate average error rate 3.8×10^{-4} and two-qubit gate error rate 6.4×10^{-3} [8]. A lower score is preferred as it implies smaller overall error rates and better fidelity of a quantum circuit. And we use the score to select the output program (quantum circuit) that represents the performance of a benchmark on a given architecture.

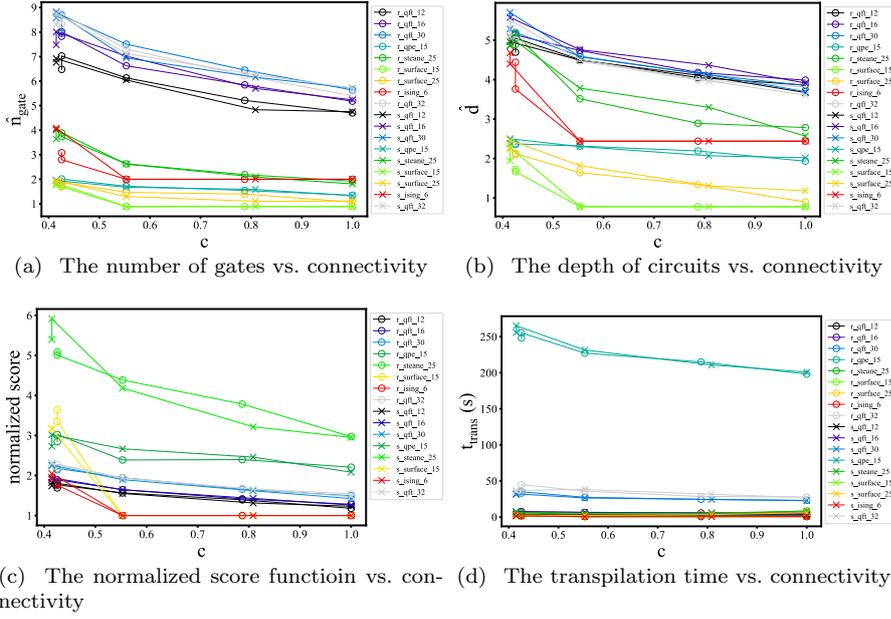## 3 Result Analysis and discussion

In this section, we evaluate the impact of qubit connectivity and topology on the performance. By defining the native gates on all target architectures identical to the typical IBM Q devices, this work ignores the impact of native gates. Through the steps described in Sec. 2, we run the Qiskit transpiler on a set of benchmark programs for ten representative architectures, select the best output, and then run the Qiskit simulator on them. In this experiment we collect the transpilation time t_{trans}, the normalized number of gates $\hat{n}_{gate}$, the normalized depth of the circuit $\hat{d}$, and the normalized simulation run time $\hat{t}_{sim}$. To compare the architecture-conforming program with the original program, we normalize the data by dividing the number after transpilation by the number of the original version.

All experiments are executed on an AWS EC2 x1.32xlarge instance with 4 Intel Xeon E7 8880 Haswell CPUs (128 logical cores) and 1,952GB of memory. The Operating System is AMI Linux 2 with Linux kernel version of 4.14. The Qiskit version is 0.20.1.

Intuitively, the four types of data we collect are all affected by connectivity, directly or indirectly. With reduced connectivity, the transpiler needs to work harder, thus increasing the transpilation time. When connectivity is reduced, more gates have to be inserted to swap the qubits, which also causes the increase in the circuit depth and the simulation time. The influence of topology may be less intuitive.

All of these riddles can be by answered by data shown in Fig. 3 and 4. Let us focus on the results in Fig. 3 first. We can see as the connectivity c increases, $\hat{n}_{gate}$, $\hat{d}$, normalized score functions, and t_{trans} decrease as a trend, namely the performance of the architectures with increasing connectivities becomes better and better. In Fig. 3 (a), the data of algorithm qft forms a group even they are different in the aspects of numbers of qubit and topologies. All curves belonging to qft family are above $\hat{n}_{gate} = 5$. The similar effect is also observed in Fig. 3 (b), where qft family is roughly above $\hat{d} = 4$. Since $\hat{n}_{gate}$ and $\hat{d}$ are related to the hardware optimization, this observation hints that the performance of hardware optimization is influenced by target algorithm family. A comparison between Fig. 3 (a) and Fig. 3 (b) also indicates that the sequence of the rest of algorithms does not change, from $steane\_25$ (green), $ising\_6$ (red), qpe_15 (green2), $surface\_25$ (yellow), to $surface\_15$ (green3). This shows the correlation between $\hat{n}_{gate}$ and $\hat{d}$. In other words, they are not independent factors in circuit design, thus the score function of Eq. 3 is introduced, which we used to select the output programs (quantum circuit), and we believe is a more valuable indicator in circuit design. In Fig. 3 (c), it is found that the normalized score function of each number of qubits of qft group drops monotonically as connectivity increases, respectively. In addition, it is also shown that the normalized score function drops monotonically as the number of qubits decrease, which is consistent with intuition that as the number of qubits of the benchmarking algorithms is larger, larger ratio of the chip is needed to run the benchmarking algorithms so the connectivity and topology effect is more significant. Fig. 3 (a) and Fig. 3 (b) illustrate the results in space domain of circuit design, while Fig. 3 (d) shows the performance comparison in the time domain.

When connectivity stays the same, it is not possible to draw the conclusion which topology always dominates performance based on our data. The possible reasons of this phenomena could be as follows. First, the topologies of rectangular-like and square-like are not so distinct in this work since the rectangular-like layout that we chosen has aspect ratio 2, which is not very asymmetric and not quite different from square-like one. Second, due to the limitation of computing resource and cost, we could not run all the benchmark algorithms with large number of qubits. When not all qubits are used to run the benchmarking algorithms, the topology effect could be reduced and less clear. In addition, possible noisy data points, especially for simulations taking very short time, may also add difficulty to draw the conclusion that which topology is always better. Need to emphasize, intuitively we expect some benchmarking algorithms perform better on some specific architecture (certain
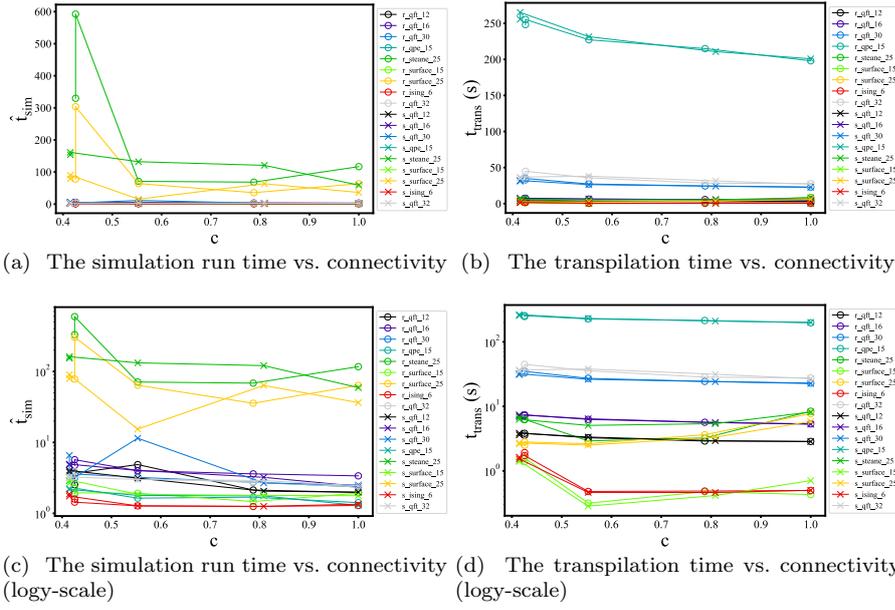
(a) The number of gates vs. connectivity

(b) The depth of circuits vs. connectivity

(c) The normalized score functioin vs. connectivity

(d) The transpilation time vs. connectivity

Fig. 3 (a) – (d) shows the experiment results of how $\hat{n}_{gate}$, $\hat{d}$, normalized score functions, and t_{trans} change with different connectivites c, respectively, by benchmarking the algorithms under different architectures (r and s are short for rectangle-like and square-like respectively). The circle markers indicate the r architectures and the cross markers indicate the s architectures. Different algorithms are labeled with different colors but the same algorithm under different architectures is labeled with the same color.

layout/topology & connectivity), and some benchmarking algorithms perform better on other specific architecture (certain layout/topology & connectivity). However, we are not making assumption that certain topology always dominates performance at different connectivity even for different benchmarking algorithms. This is consistent with our observation from the experiment data.

In Fig. 4, the effect of formation of group by algorithm family does not appear. All algorithms are mixed up. The data is more noisy in Fig. 4 (a) than that in Fig. 4 (b) since some simulation runs take very short of time which is more difficult to measure accurately. That would explain the bumpy data in Fig. 4 (a) while that in Fig. 4 (b) is more coherent. For most of the algorithms, $\hat{t}_{sim}$ and t_{trans} decreases as c increases and some of curves are quasi-linear. However, the $surface$ algorithm family does show a non-monotonic behavior in Fig. 4 (c) and (d), which means there is a possible optimal connectivity for certain specific algorithms. In terms of topology comparison, there is no dominant effect in general. But for some specific algorithms, such as qft_32, s-architecture outperforms r-architecture slightly.

In general, the impact of connectivity on performance for the same chip geometry varies up to 50% in our study by calculating and comparing the ratio of minimium and maximum values of $\hat{n}_{gate}$, $\hat{d}$, $\hat{t}_{sim}$ and t_{trans} and the ratio

(a) The simulation run time vs. connectivity

(b) The transpilation time vs. connectivity

(c) The simulation run time vs. connectivity (logy-scale)

(d) The transpilation time vs. connectivity (logy-scale)

Fig. 4 (a) and (b) show the experiment results of how the simulation run time $\hat{t}_{sim}$, and the transpilation time t_{trans} change with different connectivites c. The time performance benchmark spans in multiple orders of magnitude in time so (a) and (b) are re-plotted in logarithmic scale as (c) and (d), respectively.

can be as low as $3-5\%$. In practice, increasing connectivity and enhancing gate fidelity are often contradictory goals, so a tradeoff has to be made. Further research on noise and fidelity versus connectivity is of interest but beyond the scope of this work.

4 Conclusions and Future Work

In this work, a preliminary set of quantum benchmark algorithms for evaluating quantum chip performance is constructed, based on which the performance of superconducting quantum chip structures is quantitatively evaluated and these typical architectures are compared.

We find that connectivity plays an important role in the qubit chip design. A partially connected chip's performance is significantly lower than that of a fully connected one, and the performance difference can be several times higher. The experiment shows that quantum algorithms and circuits that use more connectivity clearly benefit from a better-connected architecture. In addition, the results suggest that co-designing quantum applications with the hardware will be paramount in successfully using quantum computers in the future. This work is mainly focused on superconducting-qubit-based quantum chips, but it can be applied to other QC implementations as well.

The connectivity in this work is analyzed quantitatively. However, it is equally crucial to quantify the topology. The topology t describes the space a chip would take, including symmetric, concentration factors etc, and the connectivity c describes fine structures in this space. Intuitively, a function of t and c may be useful to evaluate the quality of a processor, taking both of topology and connectivity into consideration. For future work, it is worthy drawing a phase diagram of performance of different benchmarking algorithms with different topology indicator t and connectivity indicator c. It would be very beneficial if some relationship or empirical formula can be established from such indicators and the quantitative parameters extracted from the benchmarking algorithms. For a certain algorithm or a set of algorithms, how to design QC chip with the optimal architecture and develop a corresponding optimized mapping algorithm to execute the algorithm with the highest possible efficiency is a topic worthy of further research.

The architectures studied are all two-dimensional lattice structures and belongs to 2-D Nearest Neighbor structure which fits in the planar layout. In the future, a three-dimensional chip architecture may become practical. Arranging connectivity in a three-dimensional architecture will be more challenging. We will further investigate how to build connectivity and make other tradeoffs in a three-dimensional architecture.

Furthermore, quantitative study on the tradeoff between connectivity and qubit quality, and supporting large-scale quantum programs on a network of quantum chips making efficient use of connectivity would be interesting topics.

Acknowledgements

Funding

Declarations

Conflict of interest

The authors declare that they have no conflict of interest.

Data availability

Data are generated using the code in via `www.github.com/sudoyang`.

Code availability

The code for this project is available in the GitHub repository found in `www.github.com/sudoyang`.

References

1. R. Barends et al. Superconducting quantum circuits at the surface code threshold for fault tolerance. *Nature*, 508(7497):500–503, April 2014. Number: 7497 Publisher: Nature Publishing Group.
2. A. D. Córcoles et al. Demonstration of a quantum error detection code using a square lattice of four superconducting qubits. *Nature Communications*, 6(1):6979, April 2015. Number: 1 Publisher: Nature Publishing Group.
3. D. Ristè et al. Detecting bit-flip errors in a logical qubit using stabilizer measurements. *Nature Communications*, 6(1):6983, April 2015. Number: 1 Publisher: Nature Publishing Group.
4. N. Ofek et al. Extending the lifetime of a quantum bit with error correction in superconducting circuits. *Nature*, 536(7617):441–445, August 2016. Number: 7617 Publisher: Nature Publishing Group.
5. M. Takita et al. Demonstration of weight-four parity measurements in the surface code architecture. *Physical Review Letters*, 117(21):210505, November 2016. arXiv: 1605.01351.
6. S. Debnath et al. Demonstration of a small programmable quantum computer with atomic qubits. *Nature*, 536(7614):63–66, August 2016. Number: 7614 Publisher: Nature Publishing Group.
7. T. Monz et al. Realization of a scalable Shor algorithm. *Science*, 351(6277):1068–1070, March 2016. Publisher: American Association for the Advancement of Science Section: Report.
8. P. Jurcevic et al. Demonstration of quantum volume 64 on a superconducting quantum computing system. *Quantum Science and Technology*, 6(2):025020, March 2021. Publisher: IOP Publishing.
9. H. Team. The world's highest performing quantum computer is here. `https://www.honeywell.com/us/en/news/2020/06/the-worlds-highest-performing-quantum-computer-is-here`. Accessed: 2021-05-12.
10. OSA. Researchers on a path to build powerful and practical quantum computer. `https://www.osa.org/en-us/about_osa/newsroom/news_releases/2020/researchers_on_a_path_to_build_powerful_and_practi/`. Accessed: 2021-05-12.
11. G. A. Q. Collaborators*† et al. Hartree-Fock on a superconducting qubit quantum computer. *Science*, 369(6507):1084–1089, August 2020. Publisher: American Association for the Advancement of Science Section: Research Article.
12. A. W. Cross et al. Validating quantum computers using randomized model circuits. *Physical Review A*, 100(3):032328, September 2019. Publisher: American Physical Society.
13. P. Smith-Goodson. Quantum volume: A yardstick to measure the performance of quantum computers. `https://www.forbes.com/sites/moorinsights/2019/11/23/quantum-volume-a-yardstick-to-measure-the-power-of-quantum-computers/?sh=1ca3c355bf4c`. Accessed: 2021-05-12.
14. M. Kjaergaard et al. Superconducting Qubits: Current State of Play. *Annual Review of Condensed Matter Physics*, 11(1):369–395, March 2020. arXiv: 1905.13641.
15. N. M. Linke et al. Experimental comparison of two quantum computing architectures. *Proceedings of the National Academy of Sciences of the United States of America*, 114(13):3305–3310, March 2017.
16. M. Y. Siraichi et al. Qubit allocation. In *Proceedings of the 2018 International Symposium on Code Generation and Optimization*, CGO 2018, pp. 113–125, New York, NY, USA, February 2018. Association for Computing Machinery.
17. A. Zulehner et al. Efficient mapping of quantum circuits to the IBM QX architectures. In *2018 Design, Automation Test in Europe Conference Exhibition (DATE)*, pp. 1135–1138, March 2018. ISSN: 1558-1101.
18. G. Li et al. Tackling the Qubit Mapping Problem for NISQ-Era Quantum Devices. In *Proceedings of the Twenty-Fourth International Conference on Architectural Support for Programming Languages and Operating Systems*, pp. 1001–1014, Providence RI USA, April 2019. ACM.

19. M. A. Nielsen and I. L. Chuang. *Quantum computation and quantum information.* Cambridge University Press, Cambridge ; New York, 10th anniversary ed edition, 2010. 00000.

20. S. Lloyd et al. Quantum algorithms for supervised and unsupervised machine learning. *arXiv:1307.0411 [quant-ph]*, November 2013. arXiv: 1307.0411.

21. N. Stamatopoulos et al. Option Pricing using Quantum Computers. *Quantum*, 4:291, July 2020. Publisher: Verein zur Förderung des Open Access Publizierens in den Quantenwissenschaften.

22. S. Ramos-Calderer et al. Quantum unary approach to option pricing. *Physical Review A*, 103(3):032414, March 2021. Publisher: American Physical Society.

23. R. B. Christensen and O. Geil. On Steane-enlargement of quantum codes from Cartesian product point sets. *Quantum Information Processing*, 19(7):192, May 2020.

24. A. G. Fowler et al. Surface codes: Towards practical large-scale quantum computation. *Physical Review A*, 86(3):032324, September 2012. Publisher: American Physical Society.

25. S. G. BRUSH. History of the Lenz-Ising Model. *Reviews of Modern Physics*, 39(4):883–893, October 1967. Publisher: American Physical Society.

26. J. Clarke and F. K. Wilhelm. Superconducting quantum bits. *Nature*, 453(7198):1031–1042, June 2008.

27. D. Kielpinski et al. Architecture for a large-scale ion-trap quantum computer. *Nature*, 417(6890):709–711, June 2002. Number: 6890 Publisher: Nature Publishing Group.

28. J. I. Cirac and P. Zoller. Quantum Computations with Cold Trapped Ions. *Physical Review Letters*, 74(20):4091–4094, May 1995. Publisher: American Physical Society.

29. A. Imamogˉlu et al. Quantum Information Processing Using Quantum Dot Spins and Cavity QED. *Physical Review Letters*, 83(20):4204–4207, November 1999. Publisher: American Physical Society.

30. L. Henriet et al. Quantum computing with neutral atoms. *Quantum*, 4:327, September 2020. Publisher: Verein zur Förderung des Open Access Publizierens in den Quantenwissenschaften.

31. K. Igeta and Y. Yamamoto. Quantum mechanical computers with single atom and photon fields. In *International Conference on Quantum Electronics (1988), paper TuI4*, pp. TuI4. Optical Society of America, July 1988.

32. F. Arute et al. Quantum supremacy using a programmable superconducting processor. *Nature*, 574(7779):505–510, October 2019. Number: 7779 Publisher: Nature Publishing Group.

33. IBM. Ibm qiskit transpiler. `https://qiskit.org/documentation/apidoc/transpiler.html`. Accessed: 2021-05-12.

34. A. Barenco et al. Elementary gates for quantum computation. *Physical Review A*, 52(5):3457–3467, November 1995. Publisher: American Physical Society.